Supporting Information for

Flexible ligand-Gd dye-encapsulated dual emission metal-organic framwork

Ya-Ru Zhang [a], Xiao-Zheng Xie [a], Xue-Bo Yin *[a,b] , and Yan Xia *[a]

[a] Tianjin Key Laboratory of Biosensing, Research Center for Analytical Science, and Molecular Recognition, College of Chemistry, Nankai University, Tianjin, 300071, China

[b] College of Chemistry and Chemical Engineering, Shanghai University of Engineering Science, Shanghai 201620, China

*xbyin@nankai.edu.cn; nkxiayan@nankai.edu.cn

Table of Contents

S1. Experiments and methods

S1.1 Reagents and materials

Dimethyl-5-hydroxyisophthalate, 1,3,5-tris (bromomethyl) benzene, rhodamine B (RhB) and gadolinium(III)) nitrate hexahydrate ($Gd(NO_3)_3 \cdot 6H_2O$) were purchased from Heowns Biochemistry Technology Co., Ltd., Tianjin, China. Potassium iodide, potassium carbonate and sodium hydroxide were get from Macklin Biochemical Co., Ltd., Shanghai, China. Copper nitrate, Ferric nitrate, Ferrous nitrate, Sodium nitrate, Chromic nitrate, Calcium nitrate, Magnesium nitrate, Nickel nitrate, Sodium fluoride, Sodium iodide, Sodium sulfite and Sodium sulfate were get from Guangfu Fine Chemistry Graduate School, Tianjin, China. N,N'-dimethylformamide, methanol, and concentrated hydrochloric acid were purchased from Concord Chemical Research Institute (Tianjin, China). All the chemicals were obtained at least of analytical grade and used without further purification. The ultrapure water used throughout all the experiments was purified through Water Purifier Nanopure water system (18.3 MΩ cm).

S1.2 Instrumentation and Characterization

NMR experiments were performed on AV 400, Bruker, America. The UV−vis absorption spectra were obtained by a UV-3600-visible spectrophotometer (Shimadzu, Japan). The fluorescence experiments were performed on a FL-4600 Fluorescence Spectrometer, Hitachi, Japan, equipped with a plotterunit and a quartz cell (1 cm × 1 cm). unit and a quartz cell (1 cm × 1 cm). Infrared spectra (IR) were obtained by Bruker TENSOR 27 Fourier transform infrared spectroscopy, over the ranging from 400 to 4000 cm^{-1}. N_2 adsorption-desorption isotherm was recorded with ASAP2020/Tristar 3000 surface area and pore analyzer at 274 K. Thermogravimetric analysis (TGA) was performed on a PTC-10ATG-DTA analyzer heated from 20°C at a ramp rate of 15°C min^{-1} under air. Powder X-ray diffraction (PXRD) patterns from an angle range of 1.5° to 50° were recorded on a D/max-2500 diffractometer (Rigaku, Japan) using Cu Kα radiation (λ = 1.5418 Å) with a scanning speed of 8° min^{-1} and a step size of 0.02° in 2θ. X-ray Photoelectron Spectroscopy (XPS) were carried out by Kratos Analytical Ltd., England.

S2. Supporting figures

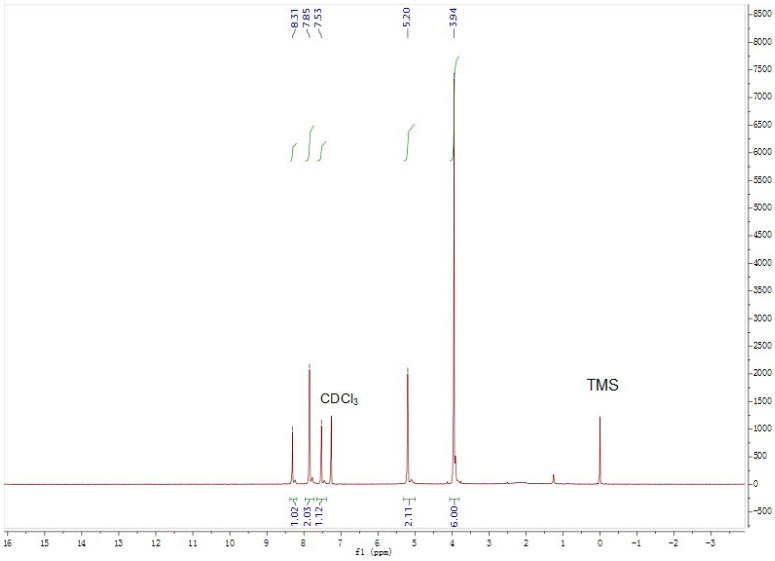

Figure S1. ^{1}H NMR spectra of **L**-COOMe

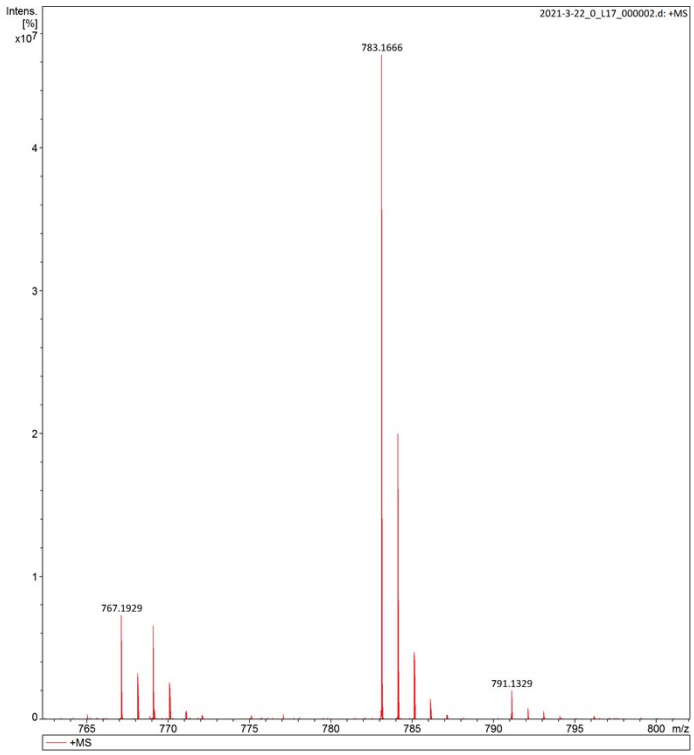

Figure S2. MS spectra of **L**-COOMe (+K)

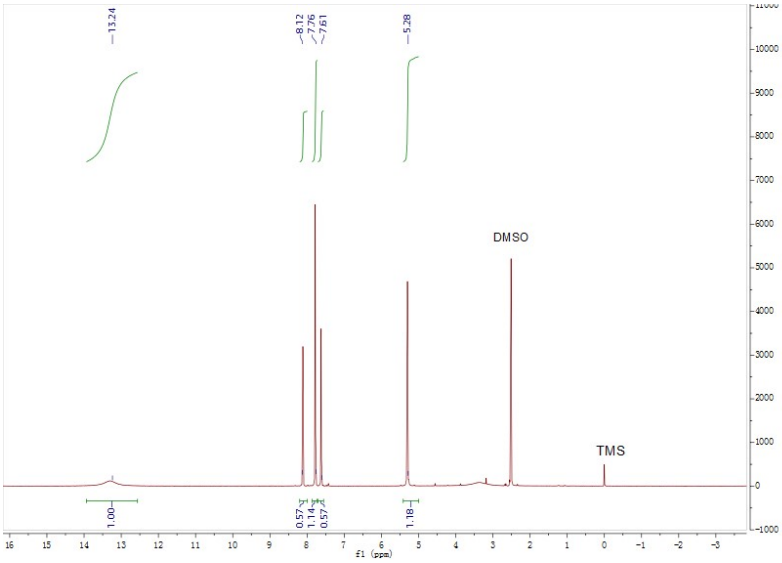

Figure S3. ^{1}H NMR spectra of **L**-COOH

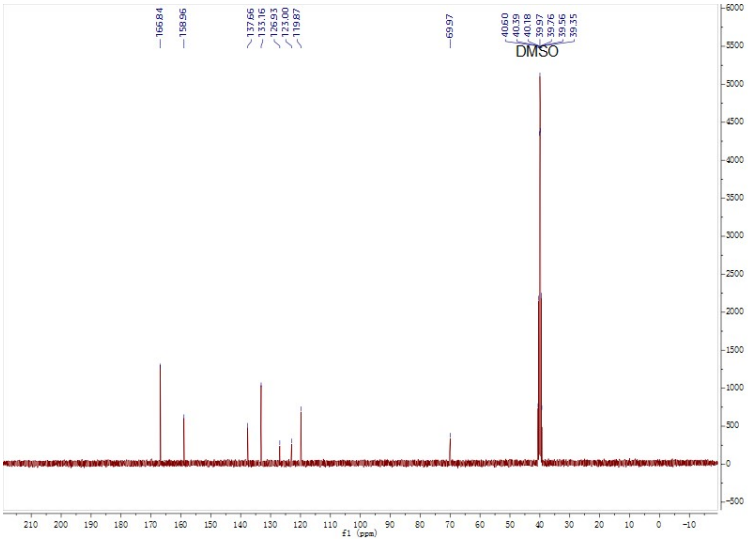

Figure S4. ^{13}C NMR spectra of **L**-COOH

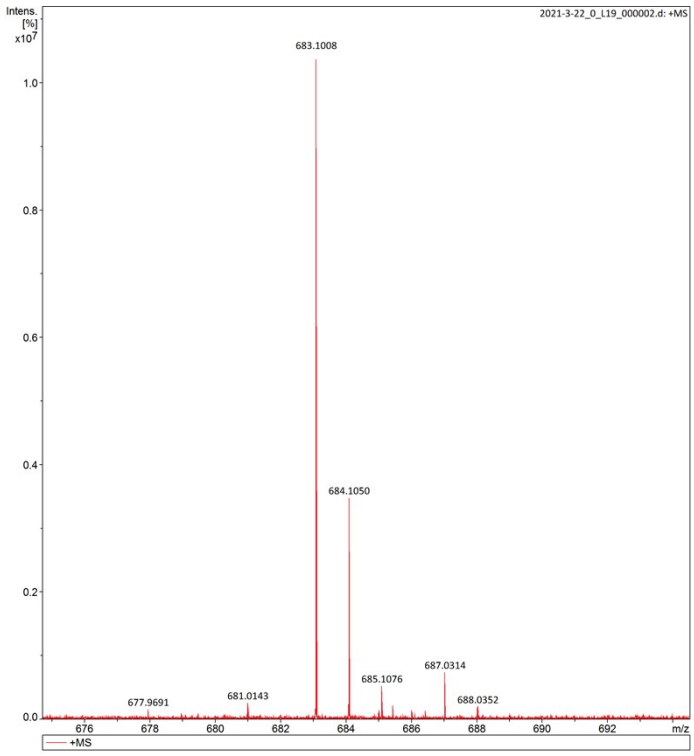

Figure S5. MS spectra of **L**-COOH (+Na)

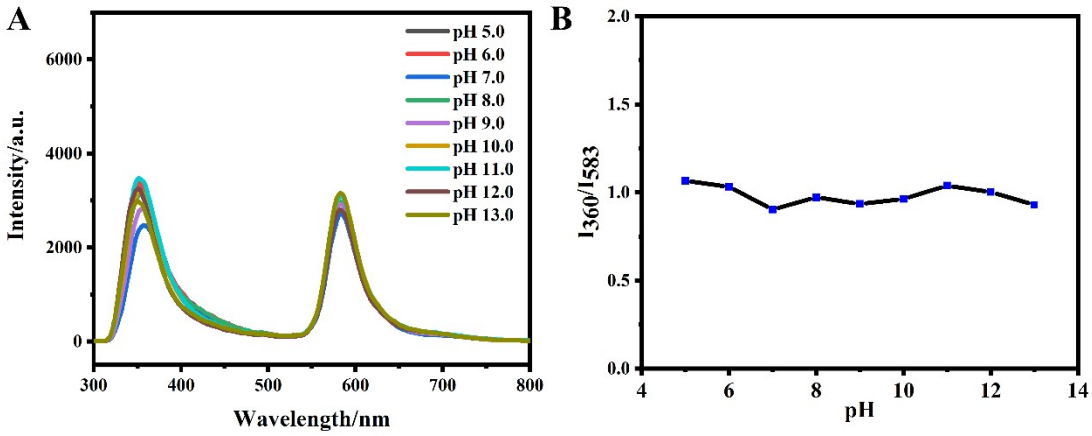

Figure S6. (A) Fluorescent spectra and (B) Fluorescence intensity ratio (I_{360}/I_{583}) of RhB@MOF in different pH values.

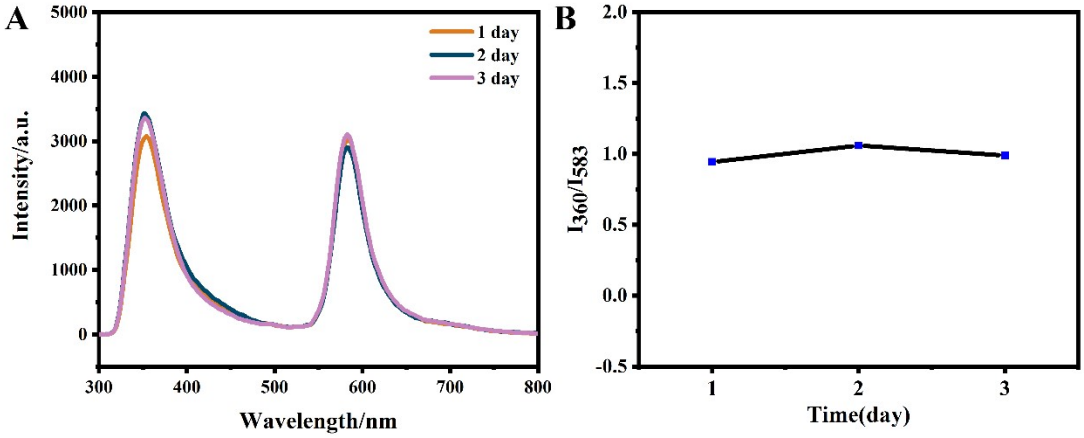

Figure S7. (A) Fluorescence spectra and (B) Fluorescence intensity ratio (I_{360}/I_{583}) of RhB@MOF in room temperature within three days under the excitation of 290 nm.

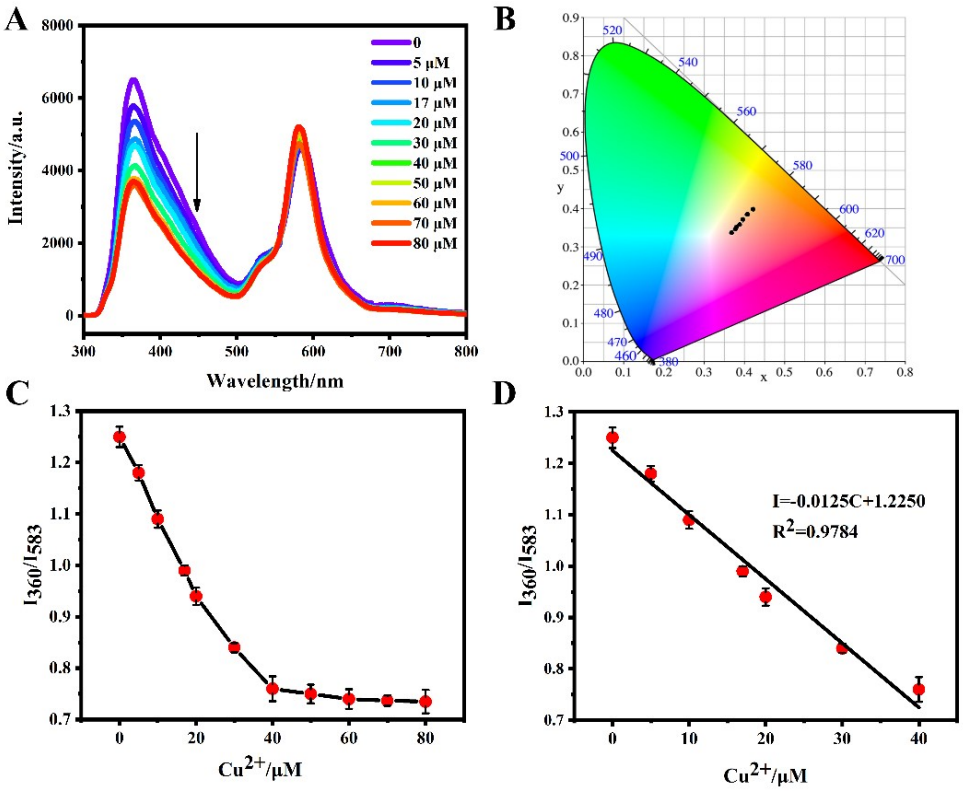

Figure S8. (A) Fluorescence spectra of RhB@MOF under different concentrations of Cu^{2+}. (B) CIE chromaticity coordinates of RhB@MOF responding to various concentration of Cu^{2+}. (C) Plot of the intensity ratio of I_{360}/I_{583} vs Cu^{2+} concentration. (D) Linear relationship between the intensity ratio of I_{360}/I_{583} and Cu^{2+} concentration.

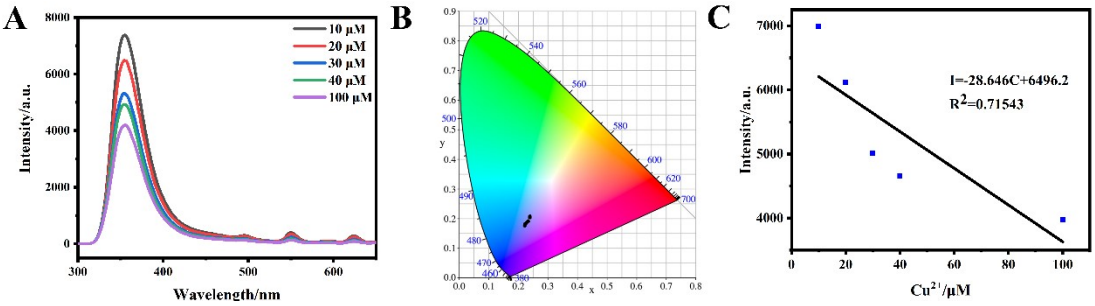

Figure S9. (A) Fluorescence spectra of MOF under different concentrations of Cu^{2+}. (B) CIE chromaticity coordinates of MOF responding to various concentration of Cu^{2+}. (C) Linear relationship between the intensity ratio of I_{360} and Cu^{2+} concentration.

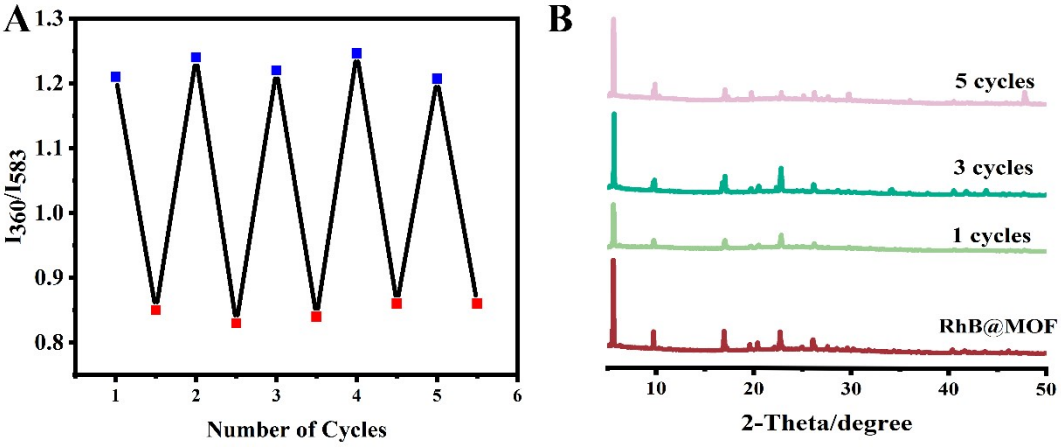

Figure S10. (A) The ratiometric fluorescence of I_{360}/I_{583} with 30 μM Cu^{2+} (blue dots) and ultrapure water (red dots). (B) PXRD patterns of RhB@MOF after five cycles with the treatment of 30 μM Cu^{2+}.

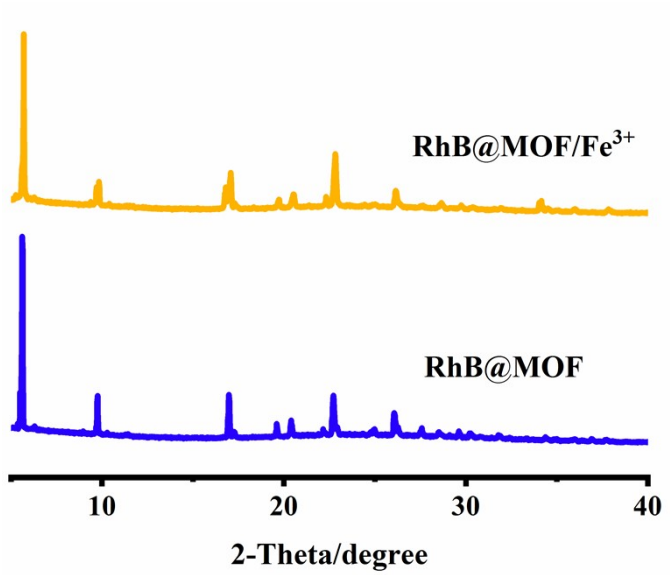

Figure S11. PXRD patterns of RhB@MOF before and after treated with Fe^{3+} aqueous solution.

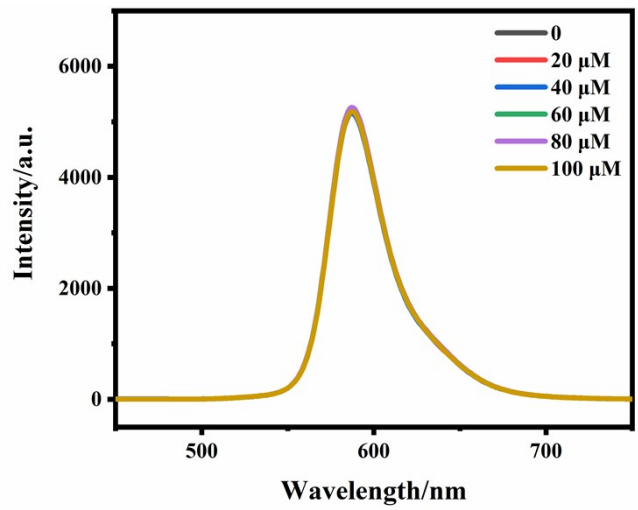

Figure S12. Fluorescence spectra of RhB under different concentrations of Cu^{2+}.

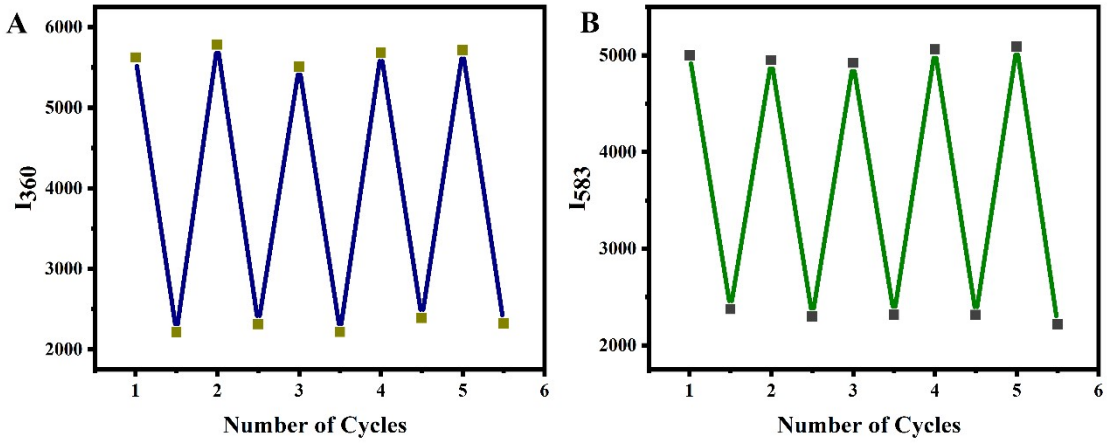

Figure S13. The emission intensity of I_{360} (A) and I_{583} (B) with Fe^{3+} aqueous solution and ultrapure water.

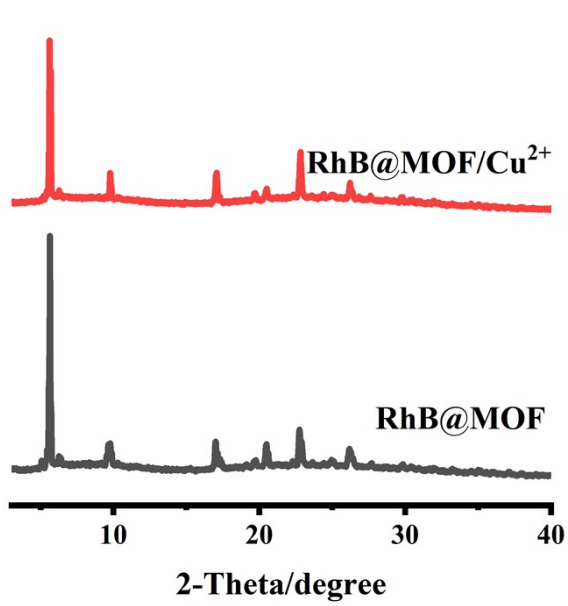

Figure S14. PXRD patterns of RhB@MOF before and after treated with Cu^{2+} aqueous solution.

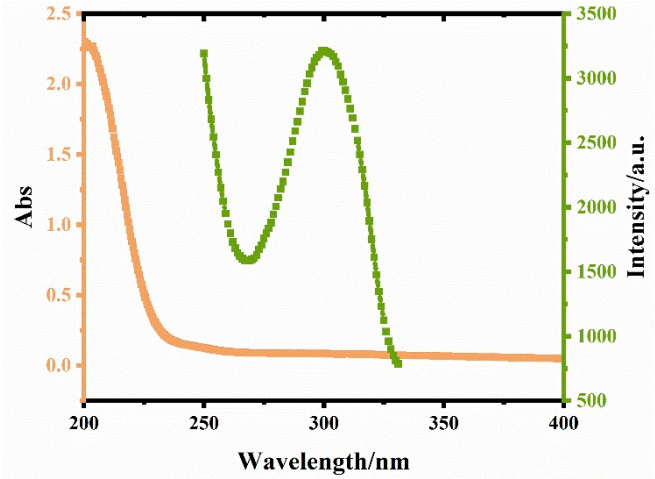

Figure S15. UV-Vis absorption spectra of Cu^{2+} and excitation spectra of MOF.

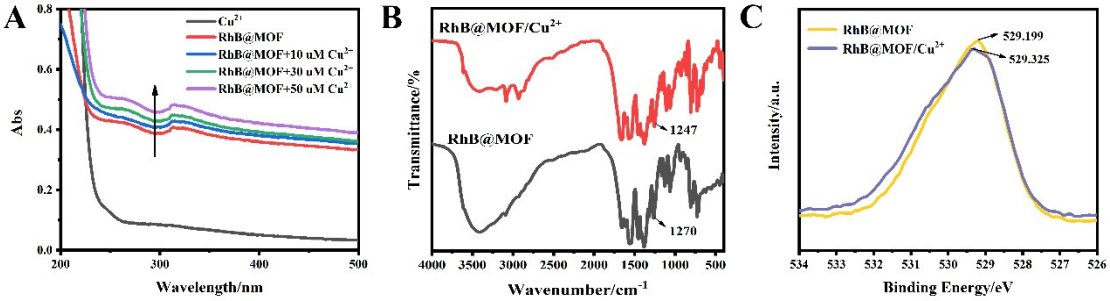

Figure S16. (A) UV-Vis absorption spectra of RhB@MOF under various concentrations of Cu^{2+}. (B) FT-IR of RhB@MOF before and after treated with Cu^{2+}. (C) O1s XPS for RhB@MOF before and after soaked in aqueous solutions of Cu^{2+}.

Table S1. Comparison of the limit of detection (LOD) for the detection of Cu^{2+} with other analytical methods.

No	Material	LOD/μM	Reference
1	RhB@MOF	0.185	this work
2	COF-JLU3	0.31	1
3	Receptor 1	7.99	2
4	BOPHY-PTZ	0.001	3
5	GA-UiO-66-NH_2	315	4
6	Eu^{3+}@Bio-MOF-1	0.14	5
7	Tb^{3+}@UiO-66-$(COOH)_2$	0.23	6
8	PQD@SiO_2	3	7
9	DPE	0.2	8

REFERENCES

1. Li, Z.; Zhang, Y.; Xia, H.; Mu, Y.; Liu, X., A robust and luminescent covalent organic framework as a highly sensitive and selective sensor for the detection of Cu(2+) ions. *Chem. Commun (Camb).* **2016,** *52* (39), 6613-6616.
2. Bhorge, Y. R.; Chou, T. L.; Chen, Y. Z.; Yen, Y. P., New coumarin-based dual chromogenic

probe: Naked eye detection of copper and silver ions. *Sensor. Actuat. B-Chem.* **2015,** *220*, 1139-1144.

3. He, C.; Zhou, H.; Yang, N.; Niu, N.; Hussain, E.; Li, Y.; Yu, C., A turn-on fluorescent BOPHY probe for Cu^{2+} ion detection. *New. J. Chem.* **2018,** *42* (4), 2520-2525.
4. Lu, M.; Deng, Y.; Luo, Y.; Lv, J.; Li, T.; Xu, J.; Chen, S. W.; Wang, J., Graphene Aerogel-Metal-Organic Framework-Based Electrochemical Method for Simultaneous Detection of Multiple Heavy-Metal Ions. *Anal. Chem.* **2019,** *91* (1), 888-895.
5. Weng, H.; Yan, B., A Eu(III) doped metal-organic framework conjugated with fluorescein-labeled single-stranded DNA for detection of Cu(II) and sulfide. *Anal Chim Acta* **2017,** *988*, 89-95.
6. Peng, X. X.; Bao, G. M.; Zhong, Y. F.; He, J. X.; Zeng, L.; Yuan, H. Q., Highly selective detection of Cu(2+) in aqueous media based on Tb(3+)-functionalized metal-organic framework. *Spectrochim. Acta. A. Mol. Biomol. Spectrosc.* **2020,** *240*, 118621.
7. Xue, W.; Zhong, J.; Wu, H.; Zhang, J.; Chi, Y., A visualized ratiometric fluorescence sensing system for copper ions based on gold nanoclusters/perovskite quantum dot@SiO_2 nanocomposites. *Analyst.* **2021,** *146* (24), 7545-7553.
8. Jiang, H.; Li, Z.; Kang, Y.; Ding, L.; Qiao, S.; Jia, S.; Luo, W.; Liu, W., A two-photon fluorescent probe for Cu^{2+} based on dansyl moiety and its application in bioimaging. *Sensor. Actuat. B-Chem.* **2017,** *242*, 112-117.